Interactions of Substrate and Product Radicals with Co^{II} in Cobalamin and with the Active Site in Ethanolamine Deaminase, Characterized by ESE-EPR and ^{14}N ESEEM Spectroscopies

Shyue-Chu Ke and Kurt Warncke*

Contribution from the Department of Physics, Emory University, Atlanta, Georgia 30322

Received February 8, 1999. Revised Manuscript Received July 2, 1999

Abstract: Interactions of the cryotrapped 2-aminopropanol-1-yl substrate radical and aminoethanol-derived product radical catalytic intermediates with the active site of vitamin B$_{12}$ coenzyme-dependent ethanolamine deaminase from *Salmonella typhimurium* in disordered frozen aqueous solution have been characterized by using X-band electron spin–echo electron paramagnetic resonance (ESE-EPR) and electron spin–echo envelope modulation (ESEEM) spectroscopies performed at 6 K. ESE-EPR spectra show that the doublet splitting of the radical line shape by electron–electron exchange and dipolar interactions with Co^{II} in cob(II)alamin is stronger for the substrate radical (11.1 mT) than for the product radical (7.1 mT). The aminoethanol-derived product radical unpaired spin density at C$_2$ is therefore positioned closer to Co^{II} than the 2-aminopropanol-1-yl substrate radical unpaired spin density at C$_1$. Multifrequency three-pulse ESEEM spectra obtained at $g = 2.00$ for each radical display the same τ- and magnetic field-dependent five-line pattern of narrow features. This indicates that the substrate and product radicals are comparably coupled to the same ^{14}N nucleus. ESEEM simulations give the following best-fit principal hyperfine tensor and nuclear quadrupole coupling parameters: **A** = [$-1.1, -0.8, -0.8$] MHz; $e^2qQ/h = 3.05$ MHz; $\eta = 0.51$. The quadrupole parameters are consistent with a secondary amide nitrogen in a polypeptide bond or with the N$_{10}$ amino nitrogen in the adenine ring of 5′-deoxyadenosine. The equivalent ^{14}N coupling for each radical indicates that either the nitrogen nucleus lies along the C$_1$–C$_2$ bond bisector or the interaction responsible for the coupling moves to remain in register with the center of unpaired spin density as it shifts 1.5 Å from C$_1$ to C$_2$ in the substrate-to-product radical transformation. The longer separation distance from Co^{II} of the product versus substrate radical indicates that the principle of radical pair stabilization by separation operates continuously through the rearrangement reaction.

Introduction

Ethanolamine deaminase[1] from bacteria catalyzes the deamination of the substrate aminoethanol to products ethanal (acetaldehyde) and ammonia.[4,5] In the first step of the proposed reaction sequence, enzyme-bound vitamin B$_{12}$ coenzyme [adenosylcob(III)alamin] is homolytically cleaved to form paramagnetic low-spin ($S = \frac{1}{2}$) Co^{II} in cob(II)alamin and a 5′-deoxyadenosyl radical. As depicted in Figure 1, the 5′-deoxyadenosyl radical has been proposed[4,5] to abstract a hydrogen atom from the substrate **1**, producing an electron-deficient substrate radical, **2**. A protein-associated radical may participate in this step.[7] The electron-deficient substrate radical **2** is thus activated for rearrangement to product radical **3** or **4**.
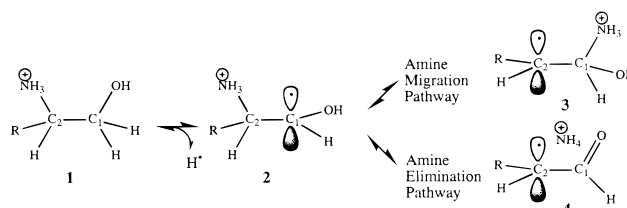

Figure 1. Depiction of substrate radical formation and proposed product radical intermediates in the rearrangement reaction catalyzed by ethanolamine deaminase. The two product radical intermediates correspond to two alternative pathways proposed for the rearrangement reaction.[4-6] The substituent R is CH$_3$ or H for 2-aminopropanol or aminoethanol substrates, respectively.

The product radical reabstracts a hydrogen atom from 5′-deoxyadenosine, forming diamagnetic product and re-forming the 5′-deoxyadenosyl radical. The basic features of cobalt–carbon bond cleavage, hydrogen atom abstractions, and substrate rearrangement are shared among members of the vitamin B$_{12}$ coenzyme-dependent enzymes.[5,8,10,11]

Ethanolamine deaminase accumulates in a Co^{II}–substrate radical pair intermediate state during steady-state turnover on

* Address correspondence to this author at Department of Physics, 1001 Rollins Research Center, 1510 Clifton Rd., Emory University, Atlanta, GA 30322. Tel.: 404-727-2975. Fax: 404-727-0873. E-mail: kwarncke@physics.emory.edu.

(1) This enzyme was originally named "ethanolamine deaminase" [2,3] (E.C. 4.3.1.7) and was later also called "ethanolamine ammonia-lyase" by some groups, in particular in the post-1970 portion of the extensive work from the laboratory of B. M. Babior.

(2) Bradbeer, C. *J. Biol. Chem.* **1965**, *240*, 4669.

(3) Kaplan, B. H.; Stadtman, E. R. *J. Biol. Chem.* **1968**, *243*, 1787–1793.

(4) Babior, B. M. In *B12*; Dolphin, D., Ed.; Wiley: New York, 1982; Vol. 2, Chapter 10.

(5) Frey, P. *Chem. Rev.* **1990**, *90*, 1343–1357.

(6) Golding, B. T. In *B12*; Dolphin, D., Ed.; Wiley: New York, 1982; Vol. 1, Chapter 15.

(7) O'Brien, R. J.; Fox, J. A.; Kopczynski, M. G.; Babior, B. M. *J. Biol. Chem.* **1985**, *260*, 16131–16136.

(8) Dolphin, D. *B12*; Wiley: New York, 1982; Vols. 1 and 2.

(9) Buckel, W.; Golding, B. T. *Chem. Soc. Rev.* **1996**, *25*, 329–338.

(10) (a) Gerfen, G. J.; Licht, S.; Willems, J.-P.; Hoffman, B. M.; Stubbe, J. *J. Am. Chem. Soc.* **1996**, *118*, 8192–8197. (b) Licht, S.; Gerfen, G. J.; Stubbe, J. *Science* **1996**, *271*, 477–481. (c) Stubbe, J.; van der Donk, W. A. *Chem. Rev.* **1998**, *98*, 705–762.

(11) Banerjee, R. *Chem. Biol.* **1997**, *4*, 175–186.

the substrate, 2-aminopropanol.[4,12] The formation rate is consistent with a kinetically competent catalytic intermediate.[12] This biradical state can be cryotrapped.[12] Cryogenic temperature electron paramagnetic resonance (EPR) spectroscopy and specific isotope labeling on 2-aminopropanol were used to show that the radical corresponds to the 2-aminopropanol-1-yl substrate radical. EPR spectral simulations showed that the substrate radical and Co^{II} in cobalamin are separated by 10−12 Å.[13] Separation of the two electron spins over a significant distance is, therefore, a central feature of the mechanism of stabilization of the radical pair against recombination before productive reaction can occur. A biradical intermediate state is also formed during turnover on the natural substrate, aminoethanol.[14,15] The radical intermediate in this state has been identified as the rearranged substrate, or product radical.[15] The structure of the product radical intermediate corresponds to either **3** or **4** in Figure 1, depending on whether rearrangement proceeds by the amine migration pathway or by the amine elimination pathway.[5,15] The mechanism of the rearrangement is unknown.[5,15]

To gain insight into the mechanisms of the radical pair separation and radical rearrangment reactions in ethanolamine deaminase from *Salmonella typhimurium*,[16] the relative separation distances from Co^{II} and active site interactions of the substrate and product radicals are addressed in these studies. Electron spin−echo (ESE) EPR[17] is used to determine the relative strength of the radical−Co^{II} electron−electron interactions from the separation distance-dependent doublet splitting of the radical line shape around $g = 2.0$. Hyperfine splittings are obscured in the EPR spectra by inhomogeneous broadening.[12,15] We have therefore used high-spectral-resolution electron spin−echo envelope modulation (ESEEM) spectroscopy[17,18] to measure hyperfine coupling of the substrate and product radicals with magnetic nuclei in the active site environment. ESEEM has previously been applied to the 2-aminopropanol-1-yl radical trapped in *Clostridium* sp. ethanolamine deaminase.[19] The results show that the separation distances of the substrate and product radicals from Co^{II} are different and that each radical is comparably coupled to an in situ ^{14}N nucleus that is based on the polypeptide or deoxyadenosine.

Experimental Section

Enzyme Preparation. Enzyme was purified from the *Eschericia coli* overexpression strain incorporating the cloned *S. typhimurium* ethanolamine deaminase coding sequences[16a] essentially as described,[16b] with the exception that the enzyme was dialyzed against buffer containing 100 mM HEPES (pH 7.45), 10 mM KCl, 5 mM dithiothreitol, 10 mM urea, and 10% glycerol.[17] Enzyme activity was assayed as described[21] by using the sensitive 3-methylbenzothiazolinone hydrazone colorimetric method for measurement of acetaldehyde produc-

tion.[22] The activity of the purified enzyme with aminoethanol as substrate was 20−30 μmol/min/mg.

Sample Preparation. The reaction was performed under dim red light in buffer containing 100 mM HEPES (pH 7.45), 10 mM potassium chloride, and 5 mM dithiothreitol. Identical results were obtained with air-saturated and anaerobic samples. Reaction was initiated by addition of adenosylcobalamin (Sigma Chemical Co.) to premixed enzyme and substrate. Reactions with 2-aminopropanol were performed at 295 K. All manipulations with aminoethanol as substrate were carried out on ice in a cold room (273 K).[15] In the different samples, the final concentration of enzyme was 20−30 mg/mL, which is equivalent to 40−60 μM for a holoenzyme molecular mass of 500 000 g/mol, or 80−120 μM active sites.[16b] Adenosylcobalamin was present at 80−120 μM (equimolar with active sites), and the concentrations of 2-aminopropanol and aminoethanol substrates were 20−30 and 100 mM, respectively. Following thorough mixing, the samples were rapidly loaded into 4 mm o.d. EPR tubes and plunged into liquid isopentane chilled with liquid nitrogen to freeze. The mixing, loading, and immersion in isopentane were accomplished in 12 s. The criteria of steady-state turnover at the time of cryotrapping are satisfied, as previously described.[15] Spin counts were performed by using 1,1-diphenylpicrylhydrazyl (DPPH) as standard. Values of 0.2 and 0.6 radicals per active site were obtained for aminoethanol and 2-aminopropanol substrates, respectively.

ESE-EPR Spectroscopy. ESE-EPR spectra were collected by using a home-constructed wideband pulsed EPR spectrometer that will be described elsewhere (K. Warncke, in preparation). The reflection microwave probe[23] featured folded half-wave microwave resonators.[24] ESE-EPR spectra were obtained by using the two-pulse microwave pulse sequence. All data processing and analysis were performed with routines written in Matlab (v. 4.2, Mathworks, Nantick, MA) and run on Silicon Graphics Indigo2 and Apple PowerPC computers.

ESEEM Spectroscopy. ESEEM was collected by using the three-pulse $(\pi/2−\tau−\pi/2−T−\pi/2)$ microwave pulse sequence,[17,18] with microwave pulse-swapping and phase-cycling.[25] τ values were selected in the three-pulse ESEEM experiments to suppress envelope modulation from matrix protons or to achieve suppression effects among the ^{14}N hyperfine modulation contributions that provide stringent constraints for the ESEEM simulations.[26,27] The τ values were sampled over the range 230−1400 ns. Envelope modulation collected for $\tau + T$ values of 0.2−5.2 μs was deadtime reconstructed[28] and Fourier transformed. Envelope modulation was also processed prior to Fourier transformation by removing the 40−60-ns amplitude trough in the pulse-crossover segment centered at τ and by correcting for the phase memory time-dominated echo decay in the modulation segment before pulse crossover. All data processing and analysis were performed with routines written by using Matlab and run on Silicon Graphics Indigo2 or PowerMacintosh computers.

ESEEM Simulations. The coupled electron−nuclear spin system of the radical was described by the following stationary-state Hamiltonian:

$$H = \beta_e \mathbf{S} \cdot \mathbf{g}_e \cdot \mathbf{B}_0 + h\mathbf{S} \cdot \mathbf{A} \cdot \mathbf{I} - g_n \beta_n \mathbf{B}_0 \cdot \mathbf{I} + \mathbf{I}' \cdot \mathbf{Q} \cdot \mathbf{I}' \qquad (1)$$

where g_e, β_e and g_n, β_n are the electron and nuclear g-value and magneton, respectively, $\mathbf{g}_e$ is the electron g-tensor, $\mathbf{B}_0$ is the external magetic field vector, h is Planck's constant, $\mathbf{A}$ is the hyperfine interaction tensor, $\mathbf{Q}$ is the nuclear quadrupole interaction tensor, and the $\mathbf{S}$ and $\mathbf{I}$ are electron and nuclear spin operators. In the strong field approximation assumed here, the electron Zeeman interaction is given by $g_e \beta_e \mathbf{B}_0 S_z'$, where S_z' is the fictitious spin operator.[29,30]

(12) Babior, B. M.; Moss, T. H.; Orme-Johnson, W. H.; Beinert, H. *J. Biol. Chem.* **1974**, *249*, 4537−4544.

(13) Boas, J. F.; Hicks, P. R.; Pilbrow, J. R. *J. Chem. Soc. Faraday Trans. 2* **1978**, *74*, 417−431.

(14) Babior, B. M.; Gould, D. C. *Biochem. Biophys. Res. Comm.* **1969**, *34*, 441−447.

(15) Warncke, K.; Schmidt, J. C.; Ke, S.-C. *J. Am. Chem. Soc.*, submitted.

(16) (a) Faust, L. P.; Connor, J. A.; Roof, D. M.; Hoch, J. A.; Babior, B. M. *J. Biol. Chem.* **1990**, *265*, 12462−12466. (b) Faust, L. P.; Babior, B. M. *Arch. Biochem. Biophys.* **1992**, *294*, 50−54.

(17) (a) Kevan, L.; Bowman, M. K. *Modern Pulsed and Continuous Wave Electron Spin Resonance*; Wiley: New York, 1990. (b) Schweiger, A. *Angew. Chem., Int. Ed. Engl.* **1991**, *30*, 265.

(18) Dikanov, S. A.; Tsvetkov, Yu. D. *Electron Spin−Echo Envelope Modulation Spectroscopy*; CRC Press: Boca Raton, FL, 1993.

(19) Tan, S. L.; Kopczynski, M. G.; Bachovchin, W. W.; Orme-Johnson, W. H.; Babior, B. M. *J. Biol. Chem.* **1986**, *261*, 3483−3485.

(20) Harkins, T. T.; Grissom, C. B. *J. Am. Chem. Soc.* **1995**, *117*, 566−567.

(21) Babior, B. M.; Li, T. K. *Biochemistry* **1969**, *8*, 154−160.

(22) Bartos, J.; Pesez, M. *Pure Appl. Chem.* **1979**, *51*, 1803−1814.

(23) Britt, R. D.; Klein, M. P. *J. Magn. Reson.* **1987**, *74*, 535−540.

(24) Lin, C. P.; Bowman, M. K.; Norris, J. R. *J. Magn. Reson.* **1985**, *65*, 396−374.

(25) (a) Fauth, J. M.; Schweiger, A.; Braunschweiler, L.; Forrer, J.; Ernst, R. R. *J. Magn. Reson.* **1986**, *66*, 74. (b) Fauth, J. M.; Schweiger, A.; Ernst, R. R. *J. Magn. Reson.* **1989**, *81*, 262.

(26) Mims, W. B. *Phys. Rev. B* **1972**, *6*, 3543.

(27) Mims, W. B.; Peisach, J. In *Advanced EPR: Applications in Biology and Chemistry*; Hoff, A. J., Ed.; Elsevier: New York, 1996; pp 1−57.

(28) Mims, W. B. *J. Magn. Reson.* **1984**, *59*, 291−306.

9924   *J. Am. Chem. Soc., Vol. 121, No. 43, 1999*

Ke and Warncke

Table 1. ESEEM Simulation Parameters[a]

A_{iso} (MHz)	A_{dip} (MHz)	e^2qQ (MHz)	η	$[\alpha, \beta, \gamma]$
0.9 ± 0.1	0.1 ± 0.1	3.05 ± 0.05	0.53 ± 0.2	45°, 170°, 45°

[a] Determination of error limits is described in the Experimental Section. The error limits on each of the Euler angles is ±5°.

The eigenvalues and eigenvectors of the electron−nuclear part of the Hamiltonian (last three terms on the right-hand side of eq 1) were obtained by separate diagonalization of the submatrix representations corresponding to the $m_s = +^1/_2$ and $m_s = -^1/_2$ electron spin manifolds. The random orientation of electron−nuclear vectors relative to the external magnetic field direction is represented by a spherical average. The pulse time domain ESEEM was simulated by direct application of the density matrix formalism of Mims.[26,31] In this formalism, the eigenvalues and eigenvectors of the electron−nuclear part of the Hamiltonian are used to determine the envelope modulation frequencies and intensities, respectively. Calculations based on the perturbation treatment of ESEEM from one member of a spin-coupled radical pair,[32] in combination with the Co[II]−2-aminopropanol-1-yl radical pair EPR simulation parameters,[13] show that the hyperfine frequencies observed in the ESEEM spectra obtained in the $g = 2$ region are shifted by less than 5% from the frequencies that would be observed in the absence of electron spin coupling. For the low-frequency features addressed in this study, these shifts are therefore within the experimental frequency resolution of 0.1−0.2 MHz. After deletion of the early envelope modulation segment corresponding to the deadtime in the experimental envelope modulation, deadtime reconstruction was performed,[28] and the envelope modulation was Fourier transformed to obtain the simulated ESEEM frequency spectrum, as in the analysis of the experimental envelope modulation. To facilitate the comparison between experimental and simulated ESEEM, the simulated modulation envelopes were multiplied by exponential decay functions derived from regression fitting of the modulation decay in the experimental envelopes. The simulations and analysis were performed with routines written by using Matlab.

In the ESEEM simulations, the variable input parameters include the diagonal hyperfine tensor, $[A_{xx}, A_{yy}, A_{zz}]$, which is the sum of an isotropic component (A_{iso}) and a point dipolar tensor, $[-A_{dip}, -A_{dip}, 2A_{dip}]$, where $A_{dip} = g_e\beta_e g_n\beta_n h^{-1} r^{-3}$ (MHz); nuclear quadrupole interaction parameters, representing the magnitude of the interaction (quadrupole coupling constant, e^2qQ) and the asymmetry (asymmetry parameter, η) of the electric field gradient at the nitrogen nucleus; and Euler angles, $[\alpha, \beta, \gamma]$, which define the mutual orientation of the nuclear quadrupole interaction tensor and hyperfine tensor principal axes. The free electron and nuclear frequencies are fixed by the experimental magnetic field value. The parameters were adjusted manually, and the best overall ("global") match of the simulated and experimental time and frequency domain data for the range of τ and magnetic field values employed was determined visually. The limits on the parameter values presented in Table 1 give the range over which the best fit was maintained.

Results

ESE-EPR Spectroscopy. Figure 2 shows two-pulse ESE-EPR spectra of the 2-aminopropanol- and aminoethanol-generated biradical states in ethanolamine deaminase, collected at 6 K. Both ESE-EPR spectra show a common broad signal with a maximum at approximately $g = 2.3$ that arises from electron spin transitions associated with Co[II] in cobalamin.[12,13] The line shape around $g = 2$, which arises from transitions associated with the substrate-derived radical, is split into a doublet by isotropic exchange and dipolar interactions of the
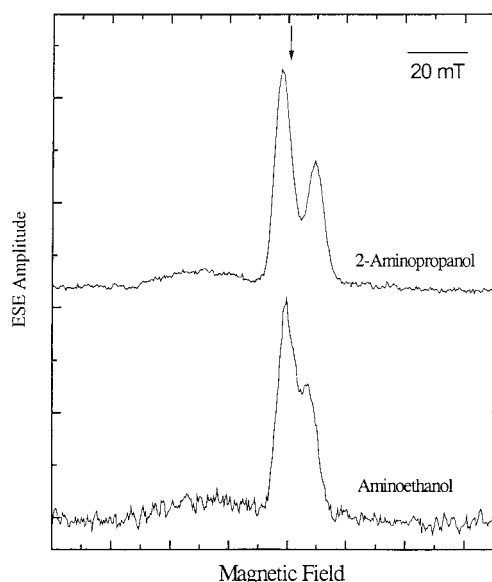
(29) Hutchison, C. A.; McKay, D. B. *J. Chem. Phys.* **1977**, *66*, 3311.
(30) Abragam, A.; Bleaney, B. *Electron Paramagnetic Resonance of Transition Ions*; Dover: New York, 1986; pp 133−178.
(31) Mims, W. B. *Phys. Rev. B* **1972**, *5*, 2409−2412.
(32) Zwanenburg, G.; Hore, P. J. *J. Magn. Reson., Ser. A* **1995**, *114*, 139−146.

Figure 2. Two-pulse ESE-EPR spectra of the biradical intermediate in ethanolamine deaminase generated by using 2-aminopropanol or aminoethanol as substrate. The arrow shows the magnetic field position at $g = 2.0$. Top, 2-aminopropanol substrate. Bottom, aminoethanol substrate. Conditions: τ, 400 ns; microwave frequency, 8.904 GHz; temperature, 6 K; microwave pulse power, 2.5 W; microwave pulse width, 100 ns; pulse sequence repetition rate, 20 Hz; 64 repetitions averaged per point; average of eight individual spectra.

radical and Co[II] electron spins.[12,13,33] The 2-aminopropanol-1-yl radical line shape displays a doublet line splitting of 11.1 mT.[34] The $g = 2$ feature of the aminoethanol-derived radical shows a smaller doublet splitting of 7.1 mT. The decrease in the doublet splitting by 36% for the aminoethanol-derived product radical shows that this radical interacts more weakly with Co[II] than the 2-aminopropanol substrate radical.

ESEEM Spectroscopy. Three-pulse ESEEM was collected for the 2-aminopropanol-derived substrate radical at selected τ values over the range 227−1316 ns at $g = 2.02$, which corresponded to maximum echo amplitude. Figures 3 and 4 show representative three-pulse ESEEM spectra obtained at the different τ values at two magnetic field values, 319.0 and 365.0 mT, respectively. The feature centered at approximately 13.6 MHz in the spectra in Figure 3 arises from weakly dipolar-coupled "matrix" protons in the environment surrounding the radical. The matrix proton feature shifts to approximately 15.5 MHz at the higher magnetic field value of 365.0 mT, as shown in Figure 4. The spectra in Figure 3 also show a pattern of narrow features with appearance of maxima at 0.8−0.9, 1.2−1.4, 1.7−2.0, 2.9−3.0, and 4.0 MHz at the different τ values. Features at 0.8, 1.8, and 2.8 MHz were previously reported for a single τ and magnetic field value in an X-band ESEEM study of *Clostridium* sp. ethanolamine deaminase.[19] Figure 4 shows that the feature at 4.0 MHz in Figure 3 increases in frequency to 4.3 MHz when the magnetic field strength is increased. In contrast, the features at 0.8−0.9, 1.7−2.0, and 2.9−3.0 MHz in Figure 3 remain at the same frequency positions to within 0.1 MHz in Figure 4. In addition, the sum of the 0.8−0.9 and

(33) Buettner, G. R.; Coffman, R. E. *Biochim. Biophys. Acta* **1977**, *480*, 495−505.
(34) The doublet splitting increases slightly with decreasing temperature below 200 K (Ke, S.-C.; Warncke, K., unpublished). The value of 9.0 mT that we obtain at 90 K by using X-band continuous-wave EPR spectroscopy is comparable to the range of values of 7.0−8.0 mT previously obtained for the *Clostridium* sp. enzyme by using X- and Q-band continuous-wave EPR spectroscopy at 93 K.[12] We are currently examining the detailed temperature dependence of the doublet splitting and line width.
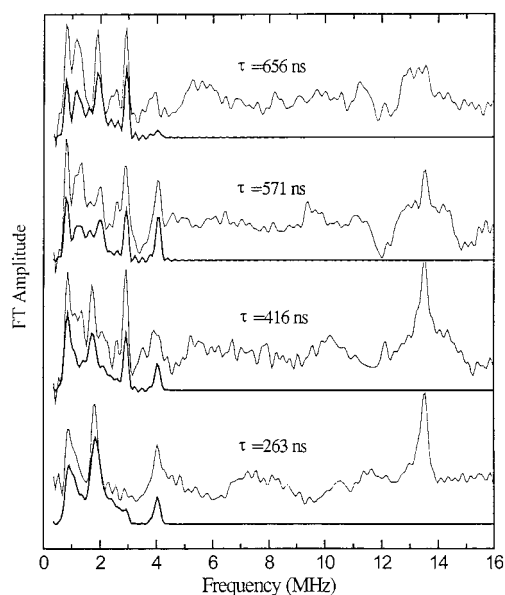
Figure 3. Experimental three-pulse ESEEM spectra and corresponding simulations for the 2-aminopropanolyl radical in ethanolamine deaminase. Spectra were obtained at $g = 2.02$ at the indicated τ value. The simulation parameters are presented in Table 1. Experimental conditions: temperature, 6 K; magnetic field, 319.0 mT; microwave frequency, 9.021 GHz; microwave pulse power, 20 W; initial T value, 200 ns; pulse width, 20 ns; pulse repetition rate, 16 Hz; 16 repetitions averaged per point.
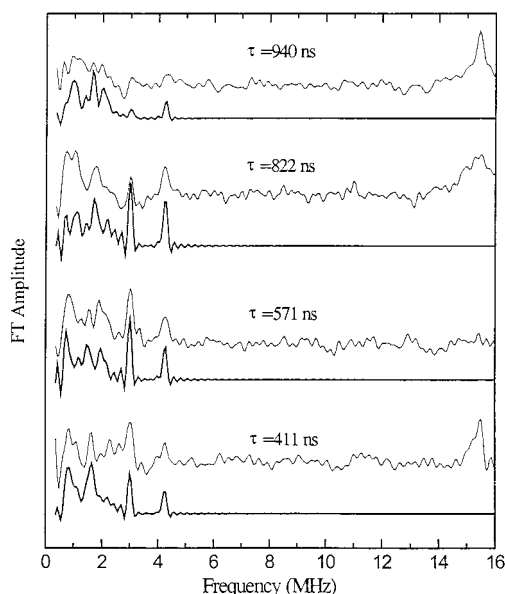

Figure 4. Experimental three-pulse ESEEM spectra and corresponding simulations for the 2-aminopropanolyl radical in ethanolamine deaminase. Spectra were obtained at $g = 2.02$ at the indicated τ value. The simulation parameters are presented in Table 1. Experimental conditions: temperature, 6 K; magnetic field, 365.0 mT; microwave frequency, 10.316 GHz; microwave pulse power, 20 W; initial T value, 200 ns; pulse width, 20 ns; pulse repetition rate, 16 Hz; 16 repetitions averaged per point.

1.7−2.0 MHz frequencies is approximately equal to the 2.9−3.0 MHz frequency.

The relative positions and magnetic field dependence of the low-frequency 2-aminopropanol-1-yl radical ESEEM spectral features are characteristic of ^{14}N coupling when the hyperfine and nuclear Zeeman contributions approximately cancel for one electron spin manifold ($A/2 \approx \nu_N$, where A is the hyperfine

coupling constant and ν_N is the free ^{14}N nuclear frequency). This creates a near zero-field, or near "exact cancellation", condition,[35,36] in which the energy level separations for one m_s state are dominated by the nuclear quadrupole interaction. We therefore assign the 0.8−0.9, 1.7−2.0, and 2.9−3.0 MHz features to the "hyperfine-adulterated" [36] ν_0, ν_-, and ν_+ nuclear quadrupole frequencies of ^{14}N. The lines are relatively narrow and do not change position appreciably with magnetic field because the nuclear quadrupole splittings arise from interaction of the ^{14}N nucleus with the electric field gradient created by the surrounding electrons.[37,38] The feature at 4.0 MHz (319.0 mT) is also characteristic of the "exact cancellation" condition. This "double quantum" feature arises from the $\Delta m_I = \pm 2$ splitting in the m_s manifold in which the hyperfine and nuclear Zeeman contributions add.[35,36] It migrates with magnetic field by twice the corresponding ^{14}N nuclear Zeeman frequency change.[35] The free ^{14}N frequencies (ν_N) at 319.0 and 365.0 mT are 0.98 and 1.12 MHz, respectively. Thus, the predicted values of $\Delta\nu_N$ and $2\Delta\nu_N$ are 0.14 and 0.28 MHz, respectively. The calculated $2\Delta\nu_N$ shift agrees with the observed shift of 0.3 MHz.

The ^{14}N features are therefore assigned to a single type of ^{14}N nucleus that is coupled to the 2-aminopropanol-derived substrate radical. The τ-dependent frequency positions and line widths of the nuclear quadrupole-dominated features, and their slight position dependence on magnetic field strength, indicate that the isotropic hyperfine and nuclear Zeeman coupling are not matched exactly and that a significant ^{14}N dipolar hyperfine interaction exists.[36] ESEEM simulations are therefore necessary to accurately specify the ^{14}N nuclear quadrupole and hyperfine coupling parameters.

Figure 5 shows a comparison of representative three-pulse ESEEM data obtained for the 2-aminopropanol- and aminoethanol-derived radicals. The signal-to-noise ratio is poorer for the aminoethanol-derived radical, because 0.2 radicals are present per active site, compared with 0.6 for the 2-aminopropanol-1-yl radical. Nevertheless, it is clear that the set of features at 0.8−0.9, 1.7−2.0, and 2.9−3.0 MHz, and the $\Delta m_I = \pm 2$ feature at 4.0 MHz, appear at the same positions and with essentially the same relative amplitudes in the spectra from each radical. The correspondence between the ^{14}N spectra at each τ value indicates that the radical−^{14}N hyperfine coupling and ^{14}N nuclear quadrupole coupling are the same for each radical within the experimental resolution. Therefore, the results indicate that the 2-aminopropanol-derived substrate radical and aminoethanol-derived product radical are coupled to the same ^{14}N nucleus.

ESEEM Simulations. Figures 3 and 4 show the simulated ESEEM spectra representing the coupling of the electron spin on the 2-aminopropanol-1-yl radical with a single ^{14}N nucleus. The simulation parameters are presented in Table 1. The simulations match well the τ- and magnetic field-dependent positions and relative amplitudes of the ^{14}N features in the experimental spectra. Thus, the simulations support the assignment of the observed coupling to a single ^{14}N nucleus.

Discussion

Origin of the Coupled Nitrogen Atom. The coupled ^{14}N nucleus could be based on the substrate, the deoxyadenosine or cob(II)alamin fragments of the coenzyme, or the protein. The weak dipolar coupling obtained in the simulations is inconsistent with a nitrogen nucleus β to the unpaired spin density centers

(35) Mims, W. B.; Peisach, J. *J. Chem. Phys.* **1978**, *69*, 4921−4930.
(36) Flanagan, H. L.; Singel, D. J. *J. Chem. Phys.* **1987**, *87*, 5606.
(37) Townes, C. H.; Dailey, B. P. *J. Chem. Phys.* **1949**, *17*, 782.
(38) Lucken, E. A. C. *Nuclear Quadrupole Coupling Constants*; Academic Press: London, 1969; Chapter 11.
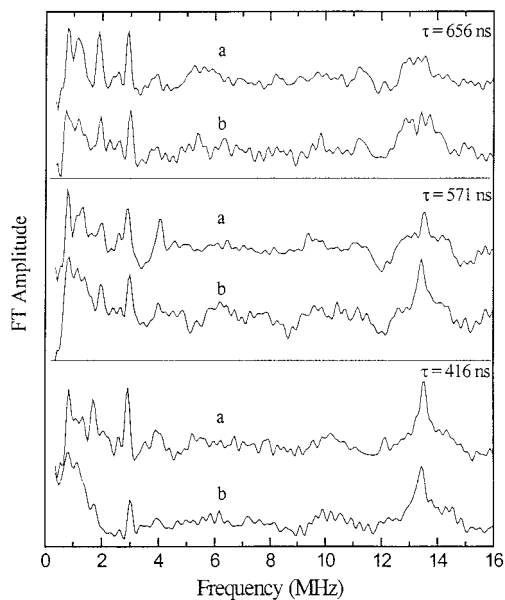
Figure 5. Comparison of three-pulse ESEEM spectra obtained for the 2-aminopropanolyl radical and the aminoethanol-derived radical in ethanolamine deaminase. (a) 2-Aminopropanolyl radical, $g = 2.02$. (b) Aminoethanol-derived radical, $g = 2.01$. The experimental conditions for the 2-aminopropanolyl radical spectra are given in the legend to Figure 3. Experimental conditions, aminoethanol-derived radical: temperature, 6 K; magnetic field, 317.0 mT; microwave frequency, 8.900 or 8.901 GHz; microwave pulse power, 20 W; initial T value, 200 ns; pulse width, 20 ns; pulse repetition rate, 16 Hz; 16 repetitions averaged per point.
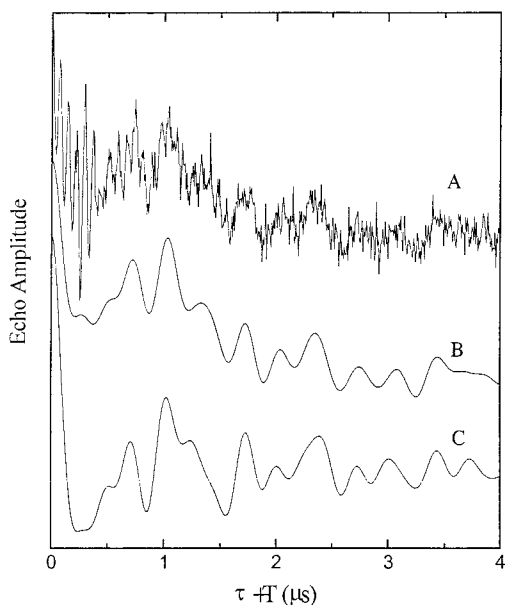

Figure 6. Experimental and simulated three-pulse ESEEM for the 2-aminopropanolyl radical. The deadtime segment of the envelope modulation has been reconstructed. (A) Experimental ESEEM collected at a τ value of 416 ns. Conditions are described in the legend to Figure 3. (B) Experimental ESEEM low-pass-filtered by inverse Fourier transformation of the complete experimental spectrum after applying a frequency cutoff of 7 MHz. (C) Simulated ESEEM for a τ value of 416 ns. Parameters are given in Table 1.

(electron$-^{14}$N nucleus separation of approximately 2 Å) in **2** and **3**, suggesting that the coupled nitrogen atom is not derived from the substrate. This corroborates the finding that generation of the biradical from ^{15}N-labeled 2-aminopropanol did not alter the ESEEM spectrum of the substrate radical.[19]
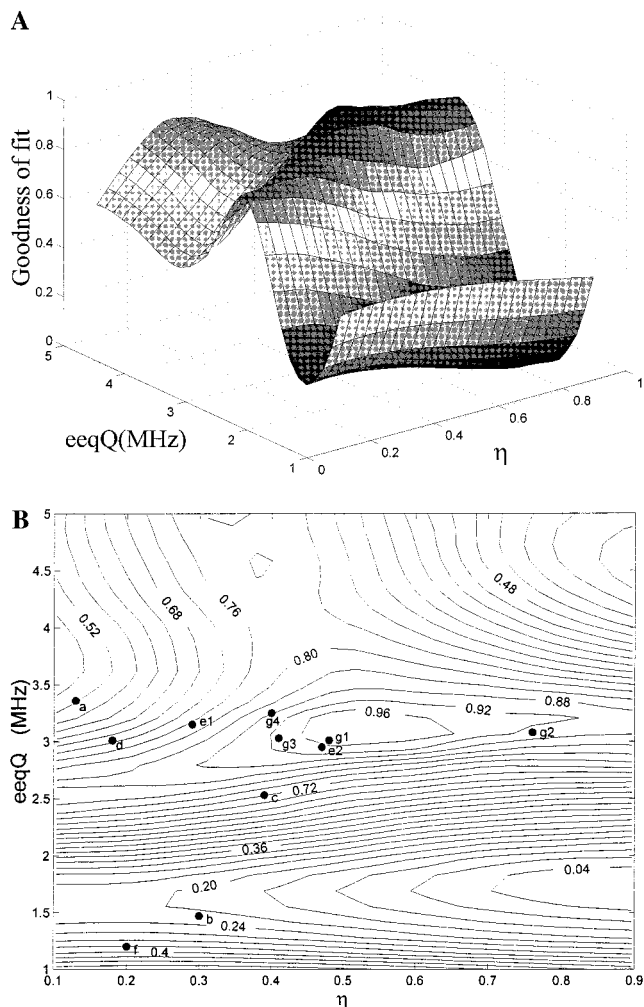

Figure 7. Goodness-of-fit of simulated to experimental ESEEM as a function of the nuclear quadrupole coupling constant and the electric field gradient asymmetry parameter. The τ value is 416 ns. (A) Surface rendition. (B) Contour plot. Overlaid points are from nuclear quadrupole coupling constants and asymmetry parameters of ^{14}N nuclei,[39] as follows: (a) histidine imidazole imino nitrogen; (b) histidine imidazole hydrochloride protonated imino nitrogen; (c) asparagine side chain primary amide nitrogen; (d) tryptophan indole nitrogen; (e1 and e2) adenine nitrogens N_7 and N_{10}, respectively; (f) polypeptide protonated α-amino nitrogen; (g1$-$g4) polypeptide secondary amide nitrogen in di- and tripeptides.

The coupled nitrogen atom can be typed by comparing the nuclear quadrupole parameters in Table 1 with parameters for ^{14}N nuclei in known bonding arrangements obtained by nuclear quadrupole resonance spectroscopic techniques.[39] This is because the nuclear quadrupole coupling constant, e^2qQ, and electric field gradient asymmetry parameter, η, are characteristic of the chemical type of ^{14}N nuclei.[38−40] To increase the accuracy of the nuclear quadrupole parameters derived from the simulations, and to better define the uniqueness of these parameters, a curve-fitting approach to matching the experimental and simulated ^{14}N envelope modulation was used. The use of fitting algorithms in matching experimental and simulated ESEEM has been mentioned previously.[41] Figure 6 shows three-pulse envelope modulation for a τ value of 416 ns at a magnetic field of 319.0 mT. The data are low-pass filtered to remove

(39) Edmonds, D. T. *Phys. Lett. C* **1977**, *29*, 233−290.

(40) The nonbonding, lone-pair electrons make the dominant contribution to the electric field gradient at the ^{14}N nucleus.[37,38] A small component of unpaired spin density in the ^{14}N p-π orbital is expected to have a minor impact on the values of e^2qQ and η relative to the diamagnetic case.

modulation from weak dipolar-coupled "matrix" protons (period $= \nu_N^{-1} = 74$ ns) that is most clearly observed in the first 0.5 μs of the recorded modulation in Figure 6A. This improves the accuracy of the fitting procedure. The filtered experimental modulation shown in Figure 6B is then fitted to a series of modulation waveforms simulated by systematically varying the values of e^2qQ and η. Figure 6C shows the best-fit modulation that produces the parameters reported in Table 1. The fit is quantitated by using the normalized sum of the squares of the residuals (χ^2) from the regression analysis as a criterion.

Figure 7 shows surface and contour renditions of goodness-of-fit as a function of e^2qQ and η. In the figure, goodness-of-fit is described by the value $1 - \chi^2$, so that a value of unity represents the best possible fit of simulation to data. The maximum in the goodness-of-fit occurs at $e^2qQ = 3.05$ MHz and $\eta = 0.53$. Goodness-of-fit values near to the maximum lie on a ridge that extends along the η dimension from $0.33 < \eta < 0.73$, which includes a variation in e^2qQ value of $3.0-3.1$ MHz. The contour plot in Figure 7 also includes literature e^2qQ and η values[39] appropriate to the intra-protein context of the coupling. The best candidates for the origin of the coupled ^{14}N are a secondary amide nitrogen in the polypeptide chain and the N_{10} amino nitrogen present in the adenine ring of the 5′-deoxyadenosine group. Tan and co-workers previously assigned the coupled ^{14}N to a polypeptide backbone nitrogen.[19] Globally ^{15}N-labeled ethanolamine deaminase is now being prepared in order to determine the polypeptide or coenzyme adenosine origin of the coupled nitrogen by using $^{15}N/^{14}N$ quotient ESEEM spectroscopy.

Comparable Coupling of the Active Site ^{14}N with the Substrate and Product Radicals. The ^{14}N hyperfine coupling parameters are the same within the experimental resolution for both the substrate and product radicals, even though, as shown in Figure 1, the radicals are distinguished by the shift of the center of unpaired spin density by the 1.5 Å carbon−carbon single bond length. The difference in interaction strength between Co^{II} and the two radicals (discussed below) suggests that the substrate-derived carbon skeleton remains stationary relative to the protein active site during the rearrangement associated with the unpaired spin density shift. Therefore, to maintain the same hyperfine interaction in the substrate radical and product radical states, either the coupled ^{14}N is positioned statically between C_1 and C_2, along the C_1-C_2 bisector, or the interaction responsible for the coupling moves to remain in register with the center of unpaired spin density as it shifts from C_1 to C_2 upon rearrangement.

Relative in Situ Position and Electron Spin−Spin Interactions between Co^{II} and the Substrate and Product Radicals. The doublet splitting of the radical line shape is caused by

exchange and dipolar interactions of the carbon-based unpaired electron spin with the unpaired electron spin on Co^{II} in cobalamin.[13,33] Both the exchange and dipolar interactions depend on the separation distance between Co^{II} and the radicals. In general, exchange coupling exhibits an exponential decrease with increased separation distance.[42] The dipolar coupling displays an inverse-cube dependence on separation distance in the point dipole limit,[43] appropriate for the $10-12$ Å separation of the unpaired spins on the 2-aminopropanol-1-yl radical and Co^{II}.[13] Therefore, the relative magnitude of the doublet splitting qualitatively indicates the relative separation distance of the radical from Co^{II}. The doublet splitting for the 2-aminopropanol-derived and aminoethanol-derived radicals are 11.1 and 7.1 mT, respectively. Therefore, the substrate radical is positioned closer to Co^{II} in cobalamin than the product radical.

The $10-12$ Å separation of the substrate radical and Co^{II} in the biradical state of ethanolamine deaminase[13] shows that establishment of a significant separation between the two electrons is an important feature of radical pair stabilization against recombination prior to rearrangement. We propose that the positions of the unpaired electron spin density in the substrate and product radicals relative to Co^{II} in cobalamin are key features of this strategy. The shorter separation of Co^{II} from the substrate radical suggests that the substrate radical is, in turn, closer to the 5′-deoxyadenosyl radical carbon center that is proposed[4] to abstract the hydrogen atom that initiates the rearrangement chemistry. This allows the initial hydrogen atom abstraction reaction to participate most effectively in the covalent trapping of the radical pair-separated state. The greater distance of the product radical from Co^{II} indicates that the principle of radical pair stabilization by separation operates continuously from the initial adenosylcobalamin cobalt−carbon bond cleavage through the rearrangement step of the reaction sequence.

(41) Wirt, M. D.; Bender, C. J.; Peisach, *J. Inorg. Chem.* **1995**, *34*, 1663−1667.
(42) Jenks, W. S.; Turro, N. J. *Res. Chem. Intermed.* **1990**, *13*, 237−300.
(43) Gordy, W. In *Techniques of Chemistry, Volume XV: Theory and Application of Electron Spin Resonance*; West, W., Ed.; Wiley & Sons: New York, 1980.